Chemosphere 356 (2024) 141794

Contents lists available at ScienceDirect

Chemosphere

journal homepage: www.elsevier.com/locate/chemosphere

Non-target analysis of crude oil photooxidation products at high latitudes and their biological effects

Zachary C. Redman [a,*], Sage Robine [b], Jason Burkhead [b], Patrick L. Tomco [a]

[a] Department of Chemistry, College of Arts and Sciences, University of Alaska Anchorage, 3211 Providence Dr., Anchorage, AK 99508, USA
[b] Department of Biological Sciences, College of Arts and Sciences, University of Alaska Anchorage, 3211 Providence Dr., Anchorage, AK 99508, USA

HIGHLIGHTS

- High-latitude oil spills were simulated under Cook Inlet, AK summer conditions.
- Hydrocarbon oxidation products were characterized with orbitrap mass spectrometry.
- Hydrocarbon oxidation product AhR activity was characterized with the CALUX assay.
- Photo-products were predominantly oxidized alkyl PAHs containing 2–4 rings.
- AhR activation indicates photoproducts may pose a greater ecological risk than parent compounds.

GRAPHICAL ABSTRACT

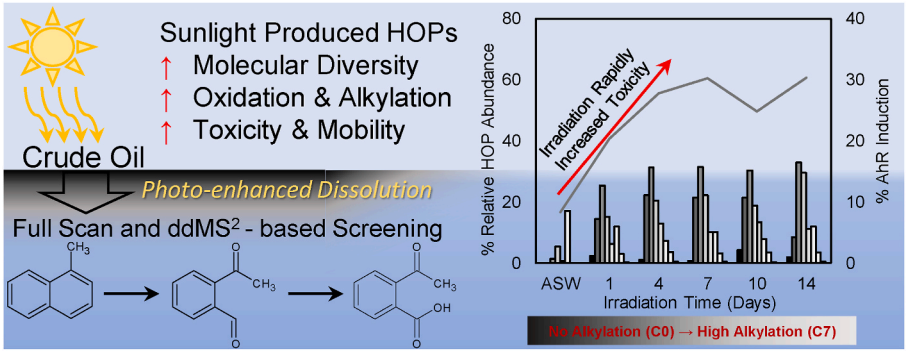

ARTICLE INFO

Handling Editor: Derek Muir

Keywords:
High-latitude oil spills
Photochemistry
High resolution orbitrap mass spectrometry
AhR CALUX assay
Oxidized polycyclic aromatic hydrocarbons
PAH
Methylated napthalaenes

ABSTRACT

With new oil and gas lease sales in high-latitude regions, there exists a need to better understand the chemical fate of spilled oil and its effects on biological life. To address this need, laboratory simulations of crude oil spills under sub-Arctic conditions were conducted using artificial seawater and exposure to solar irradiation to create Hydrocarbon Oxidation Products (HOPs). HOPs characterization and their biological effects were assessed using ultra high-performance liquid chromatography (UHPLC) with high resolution mass Orbitrap spectrometry and the aryl hydrocarbon receptor (AhR) chemically activated luciferase gene expression (CALUX) assay. Non-target UHPLC-Orbitrap mass spectrometry analysis identified 251 HOPs that were in greater abundance in light-exposed samples than dark controls. Oxidized polycyclic aromatic hydrocarbons were also detected, including phenanthrene quinone, anthraquinone, hydroxyanthraquinone, and 9-fluoreneone. The composition of HOPs were consistent with photo-products of alkylated two to four ring PAHs, primarily compounds between 1 and 3 aromatic rings and 1–3 oxygens. The HOP mixture formed during photochemical weathering of Cook Inlet crude oil induced greater AhR activity than parent petroleum products solubilized in dark controls, indicating that

Abbreviations: HOPs, hydrocarbon oxidation products; AhR, aryl hydrocarbon receptor; CALUX, chemically activated luciferase gene expression; UHPLC, ultra high performance liquid chromatography; oxyPAHs, oxidized polycyclic aromatic hydrocarbons; TPH, total petroleum hydrocarbons; TPH_d, total petroleum hydrocarbons as diesel; DRO, diesel range organics; ASW, artificial seawater; FEP, fluorinated ethylene propylene; WSF, water soluble fraction; SPE, solid phase extraction; ASET, Applied Science; Engineering, and Technology; AI_{mod}, modified aromaticity index; HCA, hierarchical clustering analysis; PCA, principal component analysis; PLSDA, partial least squares discriminant analysis; SFM, serum free media; KMD, Kendrick mass defect; VIP, variable importance in the projection.

* Corresponding author.
E-mail address: zcredman@alaska.edu (Z.C. Redman).

https://doi.org/10.1016/j.chemosphere.2024.141794
Received 22 May 2023; Received in revised form 22 December 2023; Accepted 23 March 2024
Available online 3 April 2024

HOPs, as a complex mixture, may contribute to petroleum toxicity more than the parent petroleum compounds. These non-targeted approaches provide the most comprehensive analysis of hydrocarbon oxidation products to date, highlighting the diversity of the complex mixture resulting from the photooxidation of crude oil and the limitations of targeted analyses for adequately monitoring HOPs in the environment. Taken together, these data identify a critical "blind spot" in environmental monitoring and spill clean-up strategies as there is a diverse pool of HOPs that may negatively impact human and ecosystem health.

1. Introduction

New development of oil and gas resources in high latitude regions still continue today. Such development maintains drilling activity, vessel traffic, and the potential for future crude oil spills. As rapid sea ice melt progresses globally, more shipping vessels are taking advantage of ice-free lanes to transport crude oil through remote, cold, high-latitude areas (Pizzolato et al., 2014; Dawson et al., 2015; Zhang et al., 2019; Kapsar et al., 2023) and more maritime accidents are occurring (Fedi et al., 2020). For sub-Arctic areas such as Cook Inlet, Alaska, current models of summertime marine crude oil spills predict 24% of spilled oil to remain after 30 days (BOEM, 2016). Given ample time to weather in the presence of near-continuous sunlight, dissolved hydrocarbon oxidation products (HOPs) produced during the weathering of crude oil remain overlooked in spill predictions and mitigation efforts. Continental shelf areas such as Cook Inlet have morphography, strong currents, and large tidal changes that can rapidly distribute nutrients. These characteristics are essential in supporting productive commercial and subsistence fisheries, seabirds, marine mammal populations such as critically endangered populations of beluga whales (Spies, 2006; Goetz et al., 2012). However, these same reasons, an oil spill would result in rapid dispersal of hazardous materials that could threaten marine life (Spies, 2006; Hood and Zimmerman, 1987; Royer and Grosch, 2006; Weingartner et al., 2002; Whisenhant et al., 2022).

HOPs are chemical compounds formed when spilled petroleum is photochemically and biologically weathered in the environment (Aeppli et al., 2012; Hazen et al., 2016; Townsend et al., 2003; Amos et al., 2012; McFarlin et al., 2014). These diverse pathways result in the production of a complex mixture of oxidized compounds, including oxidized polycyclic aromatic hydrocarbons (oxyPAHs), with greater water solubility and bioavailability than parent oil (Bekins et al., 2020; Essaid et al., 2011; Zito et al., 2019a; Barron, 2017; Barron and Ka'aihue, 2001; Lampi et al., 2006; Knecht et al., 2013). These compounds are potentially toxic and can diffuse large distances in the water column to impact a much larger area than predicted for parent oil (D'Auria et al., 2008; Garrett et al., 1998). At higher latitudes, exposure time to sunlight is much higher in the summer months (up to 16 h per day for sub-Arctic Cook Inlet) which could lead to the accelerated formation of oxyPAHs and other HOPs. Therefore, responses should include careful consideration of the hydrocarbon characteristics, environmental factors, and remediation tools available.

In lower latitude regions, consideration of photochemical oxidation of crude oil has become more prevalent during spill response as oxidized oil may not be as easily recovered as fresh oil (Ward et al., 2018). Other recent efforts have extended to classifying oil properties such as viscosity, water-soluble content, and interfacial tension at low temperatures with high-light conditions (Freeman et al., 2023). However, HOPs remain a "regulatory blind spot" as they fall outside the window of many standardized compliance-based analytical techniques that are used to monitor petroleum-contaminated waters and ultimately inform regulatory decisions. Quantification of total petroleum hydrocarbons (TPH), total petroleum hydrocarbons as diesel (TPHd), diesel-range organics (DRO), and/or PAHs in water is performed by solvent extraction with dichloromethane followed by gas chromatography (USEPA, 1996a, 1996b, 2000). However, none of the aforementioned methods are specific for HOPs; rather, the extraction method only captures the relatively non-polar analytes with boiling points between 170 and 430 °C (Zemo et al., 2013). Recent studies have shown that this "analytical window" misses the more-polar oxidized fraction of water-soluble petroleum (Mohler et al., 2020; Zito et al., 2019b). In contrast, recent methods of petroleum fingerprinting used to characterize HOPs in aquatic systems identify "chemical features" (e.g. condensed aromatic, aliphatic, polyphenolic, etc.) and molecular formula rather than specific compounds and associated isomers (Bianchi et al., 2014; Zhou et al., 2013; Dvorski et al., 2016; Mirnaghi et al., 2019; Whisenhant et al., 2022). These approaches include optical techniques and high-resolution mass spectrometry methods, such as fluorescence spectroscopy and Fourier transform ion cyclotron resonance mass spectrometry, which are too broad of techniques to identify specific HOPs that may warrant inclusion into target screening lists for future monitoring efforts.

Therefore, the overall goal of the project was to develop an improved method for the characterization of HOPs and establish a library of suspect compounds that correlate photochemical weathering patterns of crude oil in cold regions. Additionally, toxicological endpoints indicative of potential effects to both marine aquatic life and humans were assessed. To accomplish this, high latitude crude oil spills and progressive photo-oxidation were simulated in the laboratory such that HOPs were characterized via non-target ultra-high performance liquid chromatography (UHPLC) with high-resolution Orbitrap mass spectrometry and relative aryl hydrocarbon receptor (AhR) activation via CALUX bioassay.

2. Materials and methods

2.1. Photochemical production of hydrocarbon oxidation products in laboratory simulated oil spills

Cook Inlet crude oil was obtained from Blue Crest Energy (Anchor Point, AK) in July 2020 and stored in the dark at room temperature. The oil properties were measured by Alfa Chemistry Testing Lab (Ronkonkoma, NY) and are provided in the supporting information (Table S1). All glassware was acid-washed and combusted at 500 °C for 5 h. Water (18.2 MΩ cm) used to make artificial seawater (ASW) from Instant Ocean® (Blacksburg, VA) for experiments and for all chemical analyses was filtered to 0.22 μm. Films of crude oil at a load of 10 mg/L were added over ASW in thermostatically controlled 100 mL jacketed beakers (Chemglass USA), similar to described previously (Zito et al., 2020; Whisenhant et al., 2022; Harsha et al., 2023). Jacketed beakers were arranged in an Atlas Suntest XLS + solar simulator (1000 W xenon-arc lamp) and exposed to simulated solar irradiance of 250 W/m^2, equivalent to the peak mean monthly radiation of Southcentral Alaska summers (Dissing and Wendler, 1998) and previously documented by our group to mimic the natural solar spectrum of Southcentral Alaska (Redman et al., 2021). The photochamber air temperature was maintained at 15 °C, the lowest achievable temperature to prevent failure due to ice-buildup, using an Atlas SunCool. Each jacketed beaker was thermostatically controlled at 12 °C (typical of Cook inlet summers) and represents a single sample. Samples were prepared in triplicate and collected after 0, 1, 4, 7, 10, and 14 days. Beakers were covered with quartz lids to allow for light transmittance and secured with Teflon tape to reduce evaporation; no condensation was observed on the quartz lids over the duration of the experiments. A UV-transparent fluorinated ethylene propylene (FEP) liner (Welch fluoropolymers) was placed in each beaker to minimize adhesion of aromatic residues to each reaction

flask (Krüger et al., 2014). Dark controls were prepared identically and incubated at 12 °C in an aluminum foil-wrapped box enclosure free of light. All treatments (light and dark at each time point) were conducted in triplicate. After incubation, each sample was sacrificed and the FEP liner containing the sample was removed from the jacketed flask. The water soluble fraction (WSF) was collected by separating undissolved fuel from WSF by cutting a slit in the base and allowing the WSF to drain into a 125-mL acid-washed high density polyethylene bottle. Samples were stored at −20 °C in the dark until analyzed.

2.2. Solid phase extraction of HOPs

Total organic carbon analysis in mg/L was conducted courtesy of M. Harsha at the University of New Orleans and HOPs were concentrated to 1000 mgC/L using established methods for solid phase extraction (SPE) of dissolved organic matter, both natural and petroleum-derived, from seawater (Zito et al., 2019b; Dittmar et al., 2008). This SPE method was previously shown to have good affinity for photochemically derived oxidized petroleum residues compared to liquid extraction methods (Zito et al., 2019a, 2019b). Briefly, Agilent PPL® cartridges were pre-washed with methanol, then equilibrated with one column of water, one column of LC-MS grade methanol and one column of acidified water (0.01 N HCl) prior to loading the acidified samples (pH 1.8–2.2, ~0.01 N HCl). The entirety of a sample was loaded when insufficient volume was available to achieve 1000 mgC/L, common to dark controls and samples exposed for one day. Cartridges were rinsed with three column volumes of acidified water (0.01 N HCl) to remove salts then eluted in two fractions: 3 mL of methanol to extract polar HOPs and 15 mL of 9:1 chloroform:tetrahydrofuran to extract non-polar HOPs. Samples were then dried under nitrogen and eluted in 100 μL of methanol and transferred to 200 μL glass inserts for analysis by ultra high performance liquid chromatography tandem quadrupole high resolution orbitrap mass spectrometry. Samples were stored at −20 °C before determination of AhR activity via AhR CALUX bioassay.

2.3. Non-target UHPLC-orbitrap mass spectrometry analysis

Ultra-high performance liquid chromatography (UHPLC) with high resolution orbitrap mass spectrometry analysis of solid-phase extracted HOPs was performed at the University of Alaska Anchorage Applied Science, Engineering, and Technology (ASET) lab using a Thermo Vanquish UHPLC system coupled to an Orbitrap Exploris 120. Briefly, 5 μL of extract was injected onto a Phenomenex Kinetix C18 column (150 × 2.1 mm; 1.7 μm) and eluted using a gradient of acetonitrile and water with 0.1% formic acid. Eluted compounds were ionized with positive mode atmospheric pressure chemical ionization, previously shown to effectively ionize oxyPAHs (Grosse and Letzel, 2007), for detection via high resolution orbitrap mass spectrometry (full scan 120–800 m/z, 120, 000 resolution). Data-dependent acquisition of product ion spectra (30, 000 resolution) were collected for oxyPAHs in the in-house library and the top three most abundant precursor ions using step normalized collision energies of 40, 60, and 100 eV. Raw data files were processed using Compound Discoverer (Thermo Fisher Scientific), including chromatogram alignment, compounds detection and grouping, background removal, chemical formula assignment, and in-house library comparisons. The in-house library was developed from a mixture of thirteen available standards to provide retention times and mass spectra for oxidized PAHs of varying ring abundance and configuration, oxidation level, and functional group (carbonyl and alcohol); 1-naphthol, 2-naphthol, 9-hydroxyfluorene, 9-fluorenone, phenanthrenequinone, anthraquinone, 1,4-anthraquinone, 1-hydroxy-9, 10-anthraquinone, benzanthrone, 1-pyrenecarboxaldehyde, 1,4-chrysenequinone, 5,12-naphthacenequinone, and benzanthraquinone.

Following initial assignments, features were filtered to ensure only compounds with high peak rating (>7 in at least two replicates), mass accuracy (±1 ppm), and a product ion spectrum containing neutral mass losses indicative of oxidized functional groups (alcohols, carbonyls, and carboxylic acids) were considered. Double bond equivalents, H/C, and O/C ratios were calculated from molecular formulae to monitor the overall aromaticity and oxidation level of extracted Cook Inlet crude dissolved residues. Formulae were further classified using H/C and O/C ratios with a modified aromaticity index (AI_{mod}) as aliphatic ($H/C \geq 1.50$), unsaturated low oxygen ($AI_{mod} < 0.50$, $H/C < 1.50$, $O/C < 0.50$), unsaturated high oxygen ($AI_{mod} < 0.50$, $H/C < 1.50$, $O/C \geq 0.50$), aromatics ($0.50 \leq AI_{mod} < 0.67$), and condensed aromatics ($AI_{mod} \geq 0.67$) (Koch and Dittmar, 2006).

Peak areas were log transformed and mean-centered prior to statistical analysis using Metaboanalyst v5.0. Statistical methods included hierarchical clustering analysis (HCA), principal components analysis (PCA), and partial least squares discriminant analysis (PLSDA). PLSDA model validation and accuracy are provided in the Supporting Information (Fig. S3).

2.4. AhR CALUX bioassay

The Aryl hydrocarbon Receptor (AhR) third-generation Chemically Activated LUciferase gene eXpression (CALUX) assay was used to measure the potential of HOPs to induce biological effects. This assay has been previously applied to detect a range of chemicals in environmental extracts, including HOPs (Brennan et al., 2015; Bekins et al., 2020). Third generation stably transfected pGudLuc7.5 (an AhR-responsive luciferase reporter plasmid) rat (H4IIe7.5) and human (HepG27.5) hepatoma cell lines were generously donated by Dr. Michael S. Denison (University of California, Davis). Cells were grown in α-MEM and 400 mg/L G418 before being seeded in non-selective media in white 96-well plates at 7.5×10^4 cells/well (for H4IIe7.5's) or 1.0×10^5 cells/well (for HepG27.5's). Cells were grown to 100% confluence over 24-h for H4IIe7.5's and 72-h for HepG27.5's, then treated with 10 mgC/L of HOP extracts, determined to be the most suitable concentration for demonstrating differences in AhR activation between samples in preliminary experiments using archived photo-oxidized crude oil and diesel extracts from previous work (Supporting Information; Harsha et al., 2023). Extracts were diluted in serum-free media (SFM) for treatment. With each set of plates, a β-Naphthoflavone standard calibration curve, SPE method blank, methanol blank, SFM blank, and cell blank (i.e. no cells) were also incorporated to ensure measured bioluminescence was attributable to induction of AhR activity by HOPs. Cells were incubated with treatments for 4 h at 37 °C in an atmosphere of air with 5% CO_2 to maximize AhR activity (Bekins et al., 2020). After incubation, cells were lysed and luciferase activity was measured as described previously (Brennan and Tillit, 2018). Luciferase activity of lysates were normalized to protein concentrations of each well using the Pierce Rapid Gold BCA Protein Assay Kit. Luciferase activity per μg protein was then converted to percentage of the maximal induction by β-Naphthoflavone.

Each individual extract was analyzed in triplicate and averaged to report AhR activity of an individual sample. Data was processed in Excel. R Studio was used for the construction of protein standard curves. Statistical analysis using one-way ANOVA and Tukey's HSD for pairwise comparison was performed in JMP 16.

3. Results and discussion

3.1. Non-target analysis of photochemically produced HOPs for Cook Inlet crude oil

An increase in total non-purgeable dissolved organic carbon (NPOC) was observed over the course of the experiments in irradiated samples, indicative of the photoproduction of HOPs from Cook Inlet crude oil (Fig. 1A). Overall, 2633 chemical features were detected; primarily consisting of condensed aromatic hydrocarbons (18%), aromatic hydrocarbons (33%), and unsaturated low oxygen containing hydrocarbons (48%). A minor portion of aliphatic compounds were detected

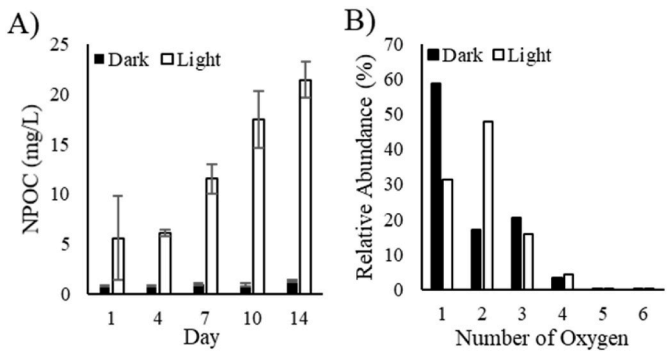

Fig. 1. Changes in DOC quantity and oxygenation. (**A**) Concentration of dissolved Non-Purgeable Organic Carbon (NPOC) with increasing oxidation time for both light and dark treated samples. Error bars represent one standard deviation. (**B**) Number of oxygen in HOP formulae identified in samples incubated in the light and dark.

(1%); however, this class of compounds was intentionally filtered from the data set in order to focus our screening efforts on oxidized aromatic compounds. Irradiated samples contained a greater relative abundance of more oxidized compounds than those incubated in the dark, further confirming the photoproduction of unique aromatic and unsaturated HOPs (Fig. 1B). Finally, 9-fluorenone, anthraquinone, 1,4-anthraquinone, and 1-hydroxy-9,10-anthraquinone were positively identified against the in-house library (minimum of two replicates) in the irradiated samples. These findings corroborate our previously reported characterization of Cook Inlet crude oil in which three-ring oxidized PAHs (anthraquinone and phenanthrenequinone) were positively identified via triple-quadrupole mass spectrometry while non-targeted analysis of HOPs showed the majority of chemical features unique to irradiated samples were oxidized condensed aromatics, aromatics, and unsaturated hydrocarbons (Harsha et al., 2023).

Our previous targeted analysis also showed high abundance of methylated naphthalenes, indicating that the targeted analysis of oxidized PAHs was limited by both the availability of analytical standards and the inherent complexity of the HOP mixture formed during the photooxidation of crude oil (Harsha et al., 2023). To investigate the presence of alkylated congeners further, Kendrick mass defects (KMD) were calculated to identify homologous series of compounds differentiated by CH_2 and determine the relative abundances of non-alkylated (C0) and potentially alkylated aromatic hydrocarbons (C1–C10) in light and dark samples (Fig. 2).

Molecular formulae were grouped by (a) number of oxygens, (b) Kendrick series, and (c) degree of alkylation for comparative purposes. For example, a chemical feature with the label "O1 Series 1" is the grouping of all molecular formula (C0–C10) in the first Kendrick series (Series 1) containing one oxygen (O1). Meanwhile, the label "O1 Series 1 C0" corresponds to a single molecular formula representative of the base formula with 0 alkyl substituents in the first Kendrick series (Series 1), containing one oxygen (O1). Using this convention, the initial KMD analysis revealed that alkylated formulae, in particular C_3H_6 (C3), are in much greater abundance than non-alkylated formulae (C0) for both irradiated samples and dark controls. Follow-on principal components analysis (PCA, Fig. 3A), partial least squares discriminant analysis (PLSDA, Fig. 3B), and hierarchical clustering analysis (HCA, Fig. 4) showed clear separation of both polar and nonpolar fractions of the irradiated and dark controlled samples. These analyses reveal that irradiated samples rapidly become chemically distinct from the dark controls with increasing irradiation time. We observe that the variability between groups is primarily due to the increased abundance of Kendrick series containing one to three oxygens within the polar fraction of sample extracts (Figs. 3C & 4D) that become present within 24 h of light exposure. This is consistent with the hypothesis that aromatic components of crude oil are oxidized to more polar, and therefore more water soluble, and potentially bioavailable, products when weathered by sunlight.

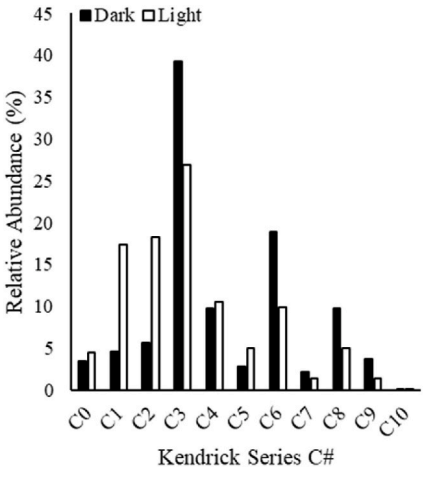

Fig. 2. Relative abundance of non-alkylated (C0) and alkylated (C1–C10) hydrocarbon oxidation products in light and dark incubated samples.

Statistical analyses were repeated to include all 2633 compounds, while the trends remain unchanged (Fig. 5A) we observe that 79% (201/255) of individual compounds with a PLSDA VIP (Variable Importance in the Projection) score greater than or equal to one fall within a Kendrick series with the top VIP scores. The majority of significant compounds were prevalent in irradiated samples (Fig. 5B), contained two oxygen (76% vs 48% relative abundance in the top VIP scores and all 2633 compounds, respectively; Fig. 5C), and were normally distributed around Kendrick group C2 (Wilks-Shapiro, W = 0.935) while the darks typically contained very low abundance compounds in the highly alkylated C8 and C9 Kendrick groups (Fig. 5D). This indicates that photo-oxidation of crude oil results in a more heterodisperse mixture of lower molecular weight oxidation products compared to non-irradiated conditions.

The significant chemical features, identified primarily in the irradiated samples, were consistent with the photochemical oxidation products of two to four ring polycyclic aromatic hydrocarbons and their alkylated derivatives (Fig. 6) (Fan et al., 2022; Nguyen et al., 2020; Luo et al., 2021).

Among the most significant compounds, 51% (130/255) belonged to two O2 Kendrick series with base formula C9H6O2 (O2 Series 8, n = 73) and C8H6O2 (O2 Series 9, n = 54) with the majority of features corresponding to Kendrick groups C0–C3 and C1–C3, respectively (Fig. 7A). The prevalence of formulae in these series are consistent with the anticipated formation of small oxidized ring opening products (Fig. 6 Boxes 19, 20, and 23) with a high degree of alkylated isomers (Fig. 8) (Luo et al., 2021). For irradiated samples, the abundance of significant HOPs peaked at ten days in the polar extracts (Fig. 7B), after which production of HOPs from crude oil likely diminishes due to a combination of limited remnant unweathered parent petroleum compounds and further degradation of HOPs to smaller products (Fig. 6 Box 45, further degradation structures not shown), as evidenced by the continuous increase in total dissolved organic carbon (Fig. 5A).

The next most abundant series contained larger compounds containing one to three oxygen with Kendrick groups C0–C4 with base formulae C13H8O3 (O3 Series 4, n = 17, Fig. 6 Boxes 35 and 41), C12H8O2 (O2 Series 6, n = 12, Fig. 6 Boxes 14 and 15), C13H8O2 (O2 Series 5, n = 10, Fig. 6 Boxes 11 and 43), and C10H8O (O1 Series 7, n = 9, naphthalene-4H-one, structure not shown); accounting for 19% (48/255) of significant features. Additional series containing compounds of higher molecular weight were also observed (6%, 15/255), including C13H8O (O1 Series 4, n = 3, Fig. 6 Box 33), C13H10O (O1 Series 5, n = 6, fluorenol, structure not shown), C14H8O3 (O3 Series 3, n = 2, Fig. 6

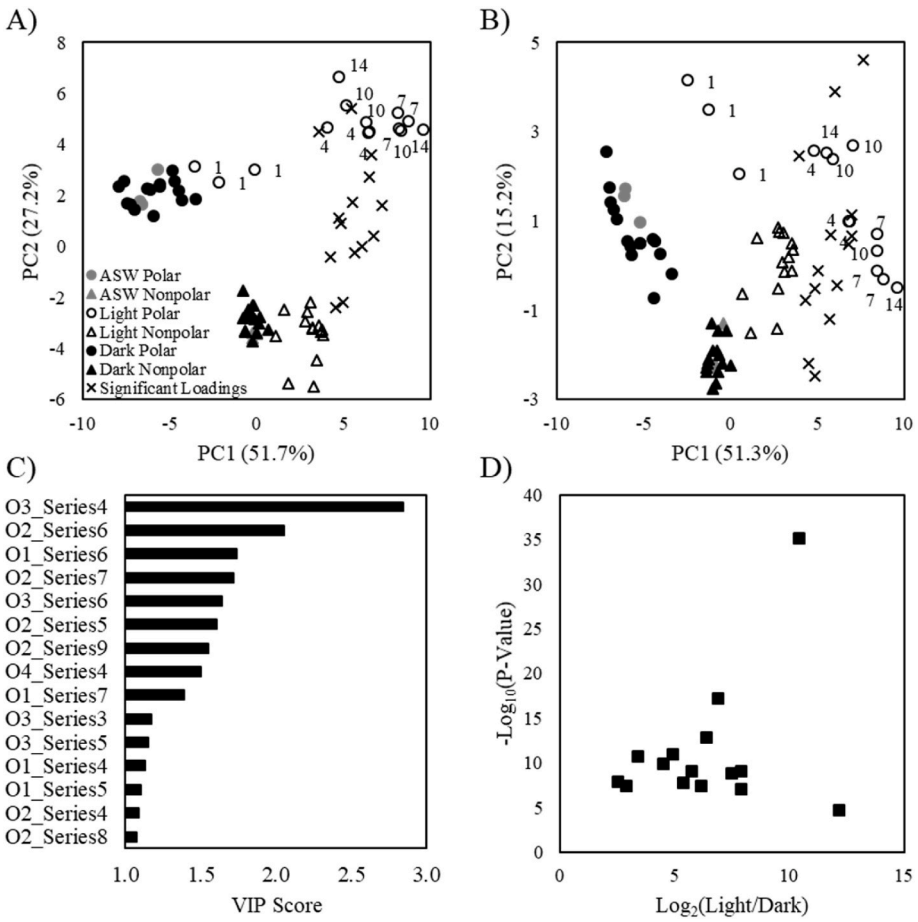

Fig. 3. (**A**) PCA and (**B**) PLSDA biplots show clear separation of light (open symbols) and dark (filled symbols) incubated samples, as well as polar (circle) and nonpolar (triangle) extracts, based upon loadings from identified Kendrick series (× 's). Artificial seawater controls (ASW, gray symbols) group with samples incubated with crude oil in the dark. Numerical labels for polar extracts of irradiated samples (open circles) indicate incubation time (days). (**C**) Variable importance in the projection (VIP) scores for the significant (VIP score >1) Kendrick series and (**D**) volcano plot show that HOP series responsible for the variation between samples are primarily composed of photooxidation products containing 1–3 oxygen. To annotate implicit features that account for the variance in the dataset, we present chemical features grouped by number of oxygens (e.g. O1, O2, etc.) and Kendrick series (Series1, Series2, etc.).

Box 12), and C15H10O2 (O2 Series 4, n = 3, Fig. 6 Boxes 4, 25, and 27). These larger, less diverse chemical species are consistent with intermediate photooxidation products of three and four ring PAHs and alkyl-PAHs including benzanthracene (Fig. 6, Compound a), 4H-cyclopenta [def]phenanthrene (Fig. 6, Compound d), anthracene (Fig. 6, Compound b), fluorene (Fig. 6, Compound e), and phenanthrene (Fig. 6, Compound f). Previous work has shown that alkylated derivatives of PAHs, particularly C1–C3, are in high abundance in crude oil and degrade quickly when subject to photoxidation (Garrett et al., 1998; Al Darouich et al., 2005). While our previous targeted efforts support this observation through the identification of oxidized anthracene and phenanthrene products, targeted analyses were limited by the complexity of the crude oil mixture stemming from the prevalence of alkylated PAHs and limited availability of analytical standards (Harsha et al., 2023). Overall, this non-targeted approach provides the most comprehensive analysis of hydrocarbon oxidation products to date, highlighting the diversity of the complex mixture resulting from the photooxidation of crude oil and the limitations of targeted analyses for adequately monitoring HOPs in the environment.

3.2. AhR activity of photochemically produced HOPs for Cook Inlet crude oil

Across the 14-day period of this study we see a trend towards increased AhR activity after one day exposed to simulated sunlight (Fig. 9). This AhR activation persists throughout the study period, indicating that degradation of crude oil by sunlight results in HOPs that persist in inducing a xenobiotic response *in vitro*. Toxicity response is likely initially driven by HOPs that significantly (VIP >1) drive the separation of light vs. dark HOP pools; largely compounds with two oxygens normally distributed around Kendrick series C2 (Fig. 5C and D). These compounds are consistent with oxidation products from the most common and acutely toxic PAHs in petroleum products which are naphthalenes (two-ring) and phenanthrenes (three-ring) (Neff, 1988; Fan et al., 2022; Nguyen et al., 2020). Since these "significant" HOPs contribute most to the differentiation of the light and dark HOP pools and we observe less AhR activation in the dark samples, it's possible that these compounds result in increased AhR activity and thus toxicity. After 10 days, AhR activity persists as the relative distribution of alkylation of significant HOPs remains unchanged up to 14 days (Fig. 9). While further degradation of HOPs results in a small decrease in the absolute abundance of significant HOPs, all samples with which cells were treated were concentrated to the same dissolved organic carbon concentration to determine AhR activity based upon sample composition rather than sample concentration. Thus, the relative distribution and AhR activation by significant HOPs remains unchanged after 14 days.

Further photooxidation of HOPs may result in compounds such as aldehydes, ketones, alcohols, peroxides and fatty acids which could also contribute to the persistence in toxicity of the day 14 samples (Neff, 1988; Fan et al., 2022; Yang et al., 2018; Nguyen et al., 2020; Lee, 2003).

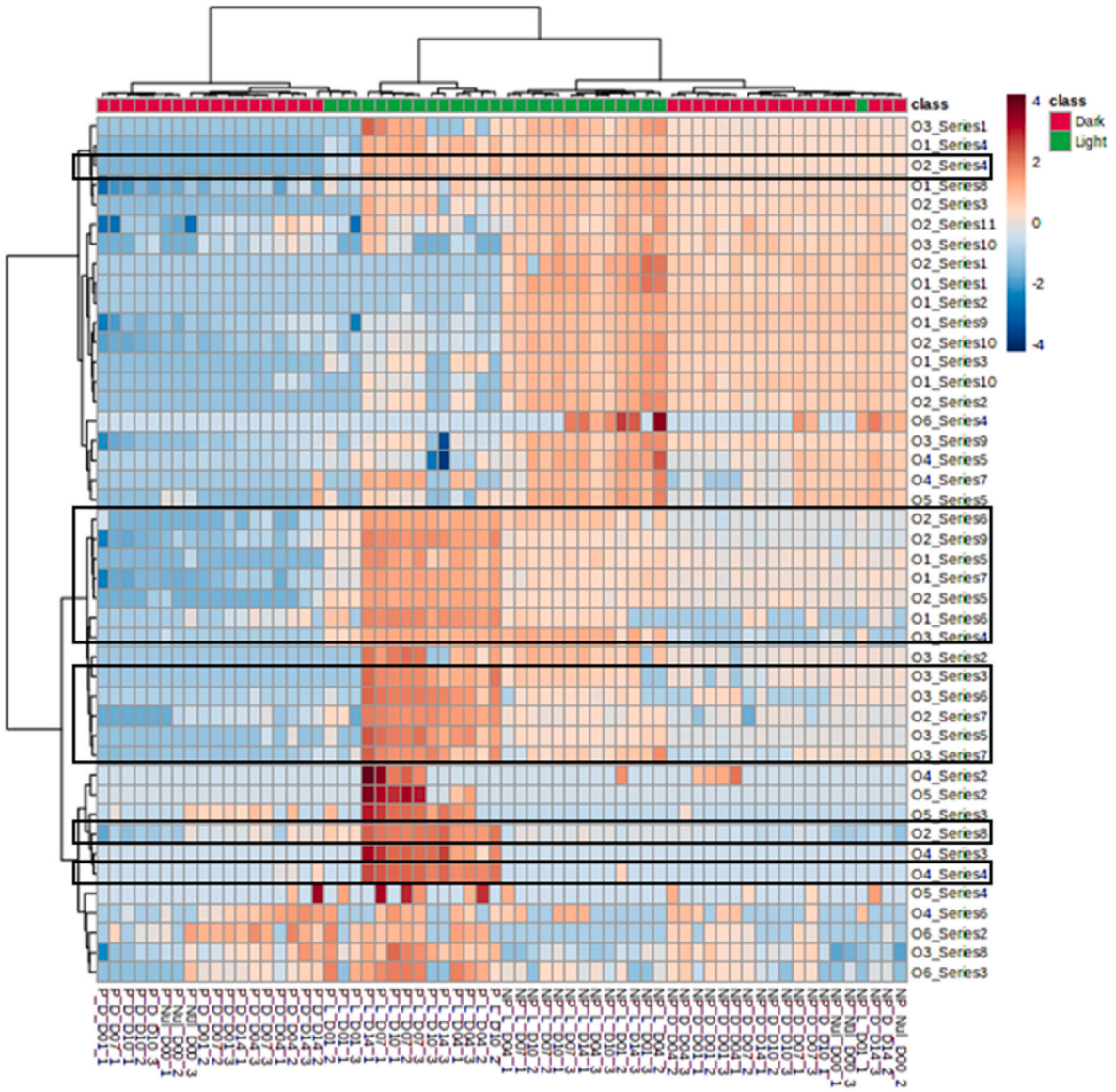

Fig. 4. Heirarchical clustering analysis (HCA) reveals distinct grouping of samples according to extract polarity (eg. polar-P vs nonpolar-NP), light exposure (eg. light-L vs dark-D), and illumination time (eg. day 1-D01 vs day 10-D10); artificial seawater controls are labeled Nul_D00. Boxes highlight Kendrick series with VIP scores greater than 1. Significant Kendrick series contain features characteristic of HOP photochemical production containing one to three oxygen that are more prevalent in the polar extracts of irradiated samples.

These types of compounds may also accumulate in dark-treated samples over time and result in AhR activity as indicated by day 14 of the study. However, as supported by our NPOC data (Fig. 1A), the naturally occurring abundance of compounds resulting in AhR activity in dark-treated samples may not be high enough to result in toxic effects. According to pilot data, a minimum concentration of approximately 5 mg C/L is required for AhR activation (Fig. S1, Supporting Information). The concentration of NPOC in dark-treated samples never exceeded 1.5 mgC/L. Similarly, a study that examined the relationship between non-volatile dissolved organic carbon concentration and sample toxicity in terms of distance from a crude oil source found that low levels (<5 mgC/L) induced minimal AhR activity and that background carbon (1.42 mgC/L) did not induce AhR activity (Bekins et al., 2020). Irradiated samples from this study accumulated up to 21.4 mgC/L on average after 14 days, which is high enough to activate AhR *in vitro* according to our preliminary study (Supporting Information). Furthermore, this concentration of dissolved organic carbon matches levels measured at other spill sites (Bekins et al., 2020; Zito et al., 2020; Bianchi et al., 2014; Lunel, 1998).

In addition to polar compounds, we treated cells with nonpolar HOP extracts for both light and dark treatments. Unfortunately, concentrating the non-polar compounds to 10 mgC/L resulted in cell death for most treatment wells. Nonpolar extracts were not available for the pilot study of the AhR CALUX bioassay (Supporting Information), so we were unaware of the increased cytotoxicity of these samples *in vitro*. Due to limited sample volume, assays could not be repeated. The composition of nonpolar extracts likely contains compounds that are more acutely toxic to cells in comparison with polar compounds. To be clear, this nonpolar fraction is composed of water-soluble HOPs that were still relatively polar compared to parent petroleum. Similarly, marine sediment extracts tested on H4IIe cells resulted in only 50–60% cell viability after treatment with non-polar compounds vs. >80% with polar compounds at the same concentration (Mennillo et al., 2020). AhR activation was also found to be strongest amongst non-polar aromatic substances, including PAHs, extracted from suspended particulate matter from flood events in Germany (Wölz et al., 2010). In particular, substances with

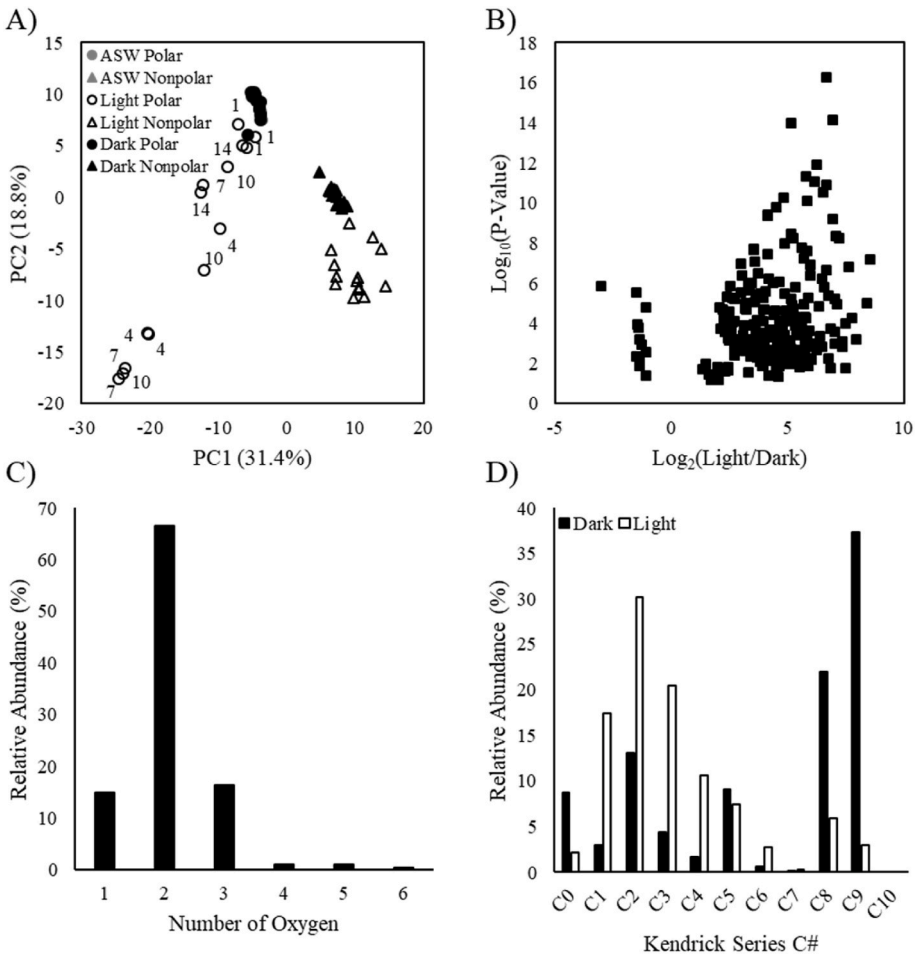

Fig. 5. (**A**) PCA scores plot for samples incorporating loadings from all 2633 detected compounds shows similar separation of light (open symbol) and dark (closed symbol) incubated samples, as well as polar (circle) and nonpolar (triangle) extracts. Artificial seawater controls (ASW, gray symbols) group with samples incubated in the dark. Numerical labels for polar extracts of irradiated samples (open circles) indicate incubation time (days). (**B**) Volcano plot of significant HOPs (VIP score >1) shows the majority are more abundant in irradiated samples. (**C**) Relative abundance of significant HOP formulae containing one to six oxygen. (**D**) Total relative abundance of non-alkylated (C0) and alkylated (C1–C10) congeners of significant HOPs in light and dark incubated samples.

more than 16 aromatic C-atoms drove the highest AhR activity. Likely the decreased availability of oxygen and exposure to sunlight of the compounds stored in the sediment of this study result in preservation of higher molecular weight PAHs which resulted in high toxicity. In comparison, our dataset focuses on oxyPAHs which may have fewer aromatic carbons, but their transformation to oxidized species still poses a potential threat as indicated by increased AhR activity after just 4 days of light exposure.

These potential toxicological effects are of concern, because it seems that the HOP pool resulting from photooxidation of crude oil persists in activating AhR for up to two weeks. Future work would benefit from increasing the duration of the experiment up to 21 days or longer to determine when toxicity of HOPs begins to decline as they are further mineralized, in addition to measurement AhR activity for identified and suspect oxyPAHs and their alkylated derivatives. AhR plays a role in xenobiotic metabolism including the cytochrome P450 (CYP450) system, which serves as a biomarker for exposure to certain environmental contaminants in addition to endogenous and exogenous drug metabolism (McDonnell and Dang, 2013; da Silva et al., 2020). For example, increased concentrations of alkylated PAHs are correlated with an increase in CYP4501A catalytic activity (including ethoxyresorufin-*O*-deethylase and methoxyresorufin-*O*-demethylase activity) in greenling fish close to oil-spill sites (Bak et al., 2019). These same PAHs also activated AhR *in vitro* at concentrations lower than those found in fish tissues *in vivo*. Similarly, bioaccumulation of PAHs in *S. rivulatus* gill and liver tissue is associated with CYP450 induction (Gaber et al., 2021). AhR bound to PAHs combines with AhR Nuclear Translocator in the nucleus to activate genes such as CYP1A1 which play a role in metabolically activating aromatic hydrocarbons into reactive metabolites (Androutsopoulos et al., 2009; Nakano et al., 2020). These metabolites can be biologically harmful leading to DNA and tissue damage (Androutsopoulos et al., 2009; Coelho et al., 2022). Thus, the AhR activation by HOPs from this study indicates a potential to result in adverse biological effects. Further studies should investigate the effects of photooxidized Cook Inet crude oil on other CYP450 biomarkers *in vitro* and *in vivo* to more specifically determine its toxicological impact.

While showing trends of increased AhR activity with photooxidation, high variation in luciferase activity between treatment replicates limited our findings of significant differences. It's possible that by highly concentrating all samples to 1000 mgC/L, the fluctuation in background dissolved organic carbon amongst samples resulted in high variation. Since samples with dark exposure and ASW controls had very little dissolved organic carbon present in the water soluble fraction, samples had to be concentrated and reconstituted in very small volumes (~6 μL). Limited sample volume meant that we did not have enough of the ASW controls and several of the dark samples to reach 10 mgC/L. Because of this issue, the day 4 dark data was removed from the dataset. To resolve the issue of limited sample volume and high background variation, future studies should test the AhR activation and toxicity of photooxidized crude oil at the concentrations that occur naturally in the

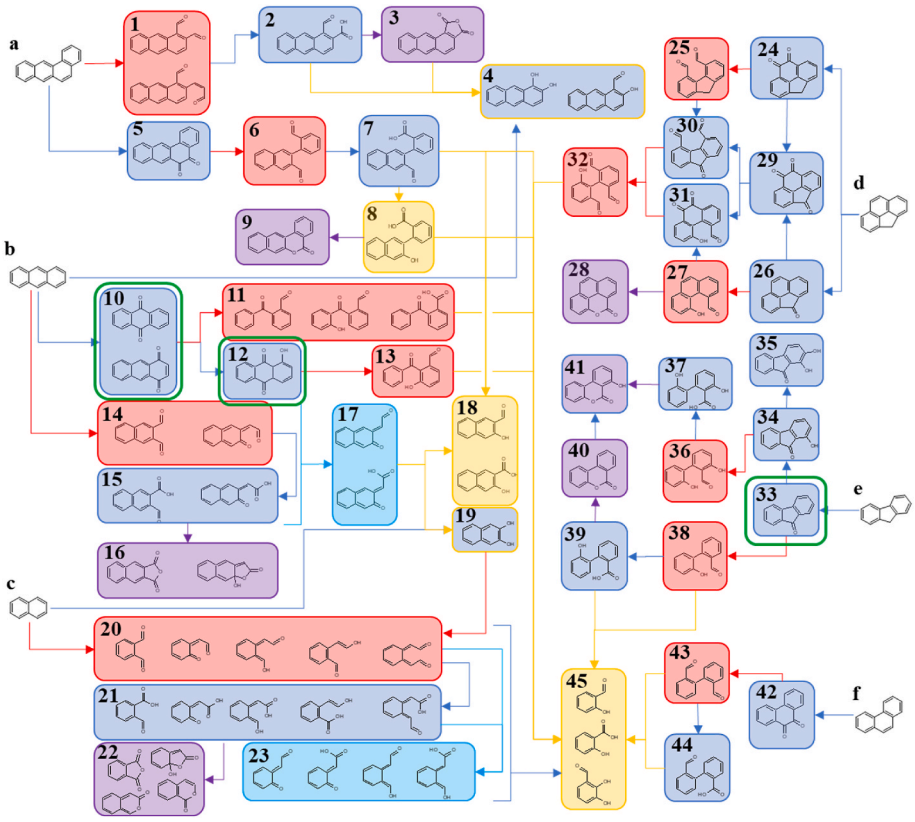

Fig. 6. Proposed HOP formation pathways (arrows) from model parent petroleum compounds benzanthracene (compound a), anthracene (compound b), naphthalene (compound c), 4H-cyclopenta[def]phenanthrene (compound d), fluorene (compound e), and phenanthrene (compound f). Bold green outlines indicate detected compounds that were matched to the in-house library. Colors indicate different chemical processes including ring opening (red), oxidation (blue), bond cleavage (gold), photoisomerization (aqua), and cyclization (purple) that may account for the production of numerous HOPs from crude oil. (For interpretation of the references to colour in this figure legend, the reader is referred to the Web version of this article.)

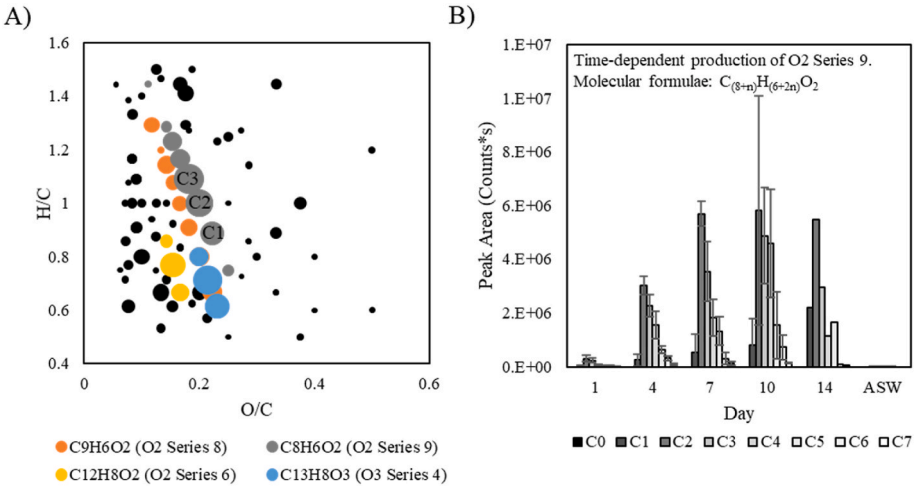

Fig. 7. (**A**) Van Krevlen diagram for significant compounds (VIP score >1) with circle size scaled to compound VIP scores. Prevalent Kendric series are highlighted and C1–C3 labels corresponding to the alkylated Kendrick groups for O2 Series 9, base formula C8H6O2 (see Fig. 6 Boxes 19, 20, and 23 for representative structures), are provided. (**B**) Average abundance (n = 3, Day 14 n = 2) of detected compounds within O2 Series 9 (molecular formulae $C_{(8+n)}H_{(6+2n)}O_2$ where n is the degree of alkylation, eg. n = 0 for C0) over time further shows the accumulation of significant HOPs peaks at ten days, with the majority of detected features present as alkylated congeners. Artificial seawater controls (ASW) confirm that significant HOP features were not detected in the absence of crude oil. Error bars represent one standard deviation.

samples. AhR activation, although strongly associated with toxicity response, is also not a guarantee of adverse health impacts. Several other studies also demonstrate the toxicity of oxyPAHs by mortality, malformations and oxidative stress in aquatic organisms (Barron, 2017; Lampi et al., 2006; Knecht et al., 2013). Future work should assess biological impacts of photooxidized Cook Inlet crude oil intermediates *in vivo*. Despite these considerations, it is clear that HOPs formed during the photooxidation of crude oil have the potential to harmfully impact

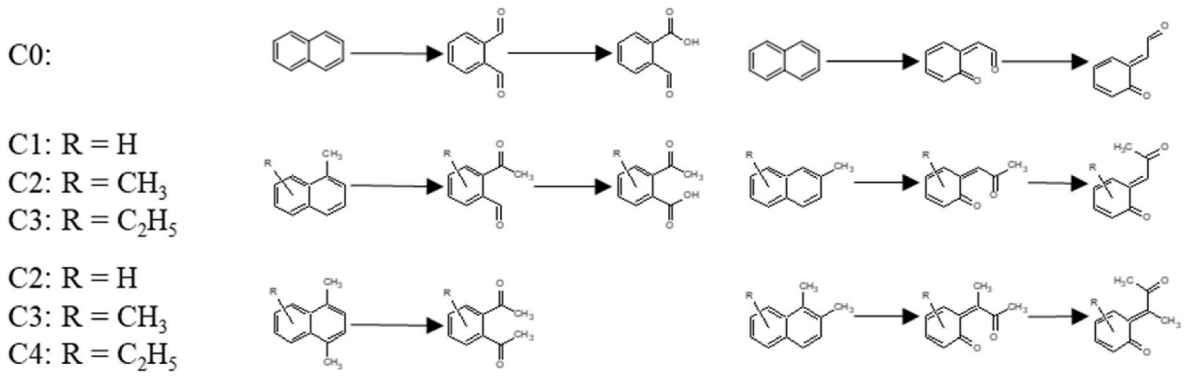

Fig. 8. Proposed general pathway for the formation of HOPs in Kendrick series with base formula C8H6O2 and C8H6O3 from model parent petroleum compound naphthalene and its methylated congeners.

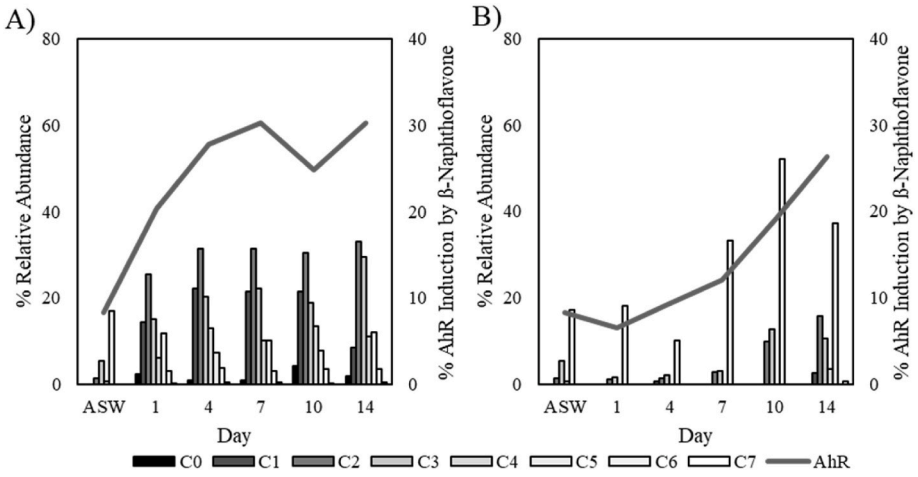

Fig. 9. Average (n = 3, (A) Day 14 n = 2) relative abundance of HOPs in Cook Inlet crude oil polar extracts incubated in the (**A**) light and (**B**) dark at each time point (bars) and the percent AhR induction relative to β-naphthoflavone of extracts concentrated to 10 mgC/L (line).

organisms; coupled with increased mobility and bioavailability relative to parent petroleum, HOPs may pose a significant ecological risk that should be considered post-spill.

4. Conclusions

This non-targeted approach provides the most comprehensive analysis of hydrocarbon oxidation products to date, highlighting the diversity of the complex mixture resulting from the photooxidation of crude oil and the limitations of targeted analyses for adequately monitoring HOPs in the environment. Our previous work concluded that targeted methods are inadequate for the characterization of petroleum residues and HOPs due to the inherent complexity of the mixture and relatively limited availability of reference standards and libraries. To address this, we developed a non-targeted analysis for HOPs formed by the photooxidation of Cook Inlet crude oil using ultra-high performance liquid chromatography coupled to orbitrap high resolution mass spectrometry. The photooxidation of Cook Inlet crude oil produces HOPs consisting primarily of condensed aromatic hydrocarbons, aromatic hydrocarbons, and unsaturated low oxygen containing hydrocarbons. Compounds from the light-treated samples had higher levels of oxidation compared to dark-treated controls with differences between the two treatment groups being primarily driven by compounds containing 1–3 oxygens and being C2-3 alkylated. These results are consistent with the photochemical oxidation products of two to four ring PAHs and their alkylated derivatives to oxyPAHs. Overall, coupled CALUX bioassays indicate that HOPs generated by photochemical weathering of Cook Inlet Crude may pose a greater ecological risk than parent petroleum compounds due to the greater mobility and bioavailability of oxidized products.

CRediT authorship contribution statement

Zachary C. Redman: Conceptualization, Data curation, Formal analysis, Investigation, Methodology, Supervision, Validation, Visualization, Writing – original draft, Writing – review & editing. **Sage Robine:** Data curation, Formal analysis, Investigation, Methodology, Validation, Visualization, Writing – original draft. **Jason Burkhead:** Conceptualization, Funding acquisition, Project administration, Resources, Validation, Writing – review & editing. **Patrick L. Tomco:** Conceptualization, Funding acquisition, Project administration, Resources, Validation, Writing – review & editing.

Declaration of competing interest

The authors declare that they have no known competing financial interests or personal relationships that could have appeared to influence the work reported in this paper.

Data availability

Data will be made available on request.

Acknowledgements

We are grateful to M. Harsha for conducting total organic carbon analysis and for funding provided by the Bureau of Ocean and Energy Management and the Coastal Marine Institute (M21AC00017). Additional support was provided to P. Tomco by the ConocoPhillips Arctic Science and Engineering Endowment and the National Science Foundation Award #1929173 and #2019123.

Appendix A. Supplementary data

Supplementary data to this article can be found online at https://doi.org/10.1016/j.chemosphere.2024.141794.

References

Aeppli, C., Carmichael, C.A., Nelson, R.K., Lemkau, K.L., Graham, W.M., Redmond, M.C., Valentine, D.L., Reddy, C.M., 2012. Oil weathering after the Deepwater Horizon disaster led to the formation of oxygenated residues. Environ. Sci. Technol. 46 (16), 8799–8807.

Al Darouich, T., Behar, F., Largeau, C., Budzinski, H., 2005. Separation and characterisation of the C15-aromatic fraction of Safaniya crude oil. Oil Gas Sci. Technol. 60 (4), 681–695.

Amos, R., Bekins, B., Cozzarelli, I., Voytek, M., Kirshtein, J., Jones, E., Blowes, D., 2012. Evidence for iron-mediated anaerobic methane oxidation in a crude oil-contaminated aquifer. Geobiology 10 (6), 506–517.

Androutsopoulos, V.P., Tsatsakis, A.M., Spandidos, D.A., 2009. Cytochrome P450 CYP1A1: wider roles in cancer progression and prevention. BMC Cancer 9, 187.

Bak, S., Nakata, H., Koh, D., Yoo, J., Iwata, H., Kim, E., 2019. In vitro and in silico AHR assays for assessing the risk of heavy oil-derived polycyclic aromatic hydrocarbons in fish. Ecotoxicol. Environ. Saf. 181, 214–223.

Barron, M.G., 2017. Photoenhanced toxicity of petroleum to aquatic invertebrates and fish. Arch. Environ. Contam. Toxicol. 73 (1), 40–46.

Barron, M.G., Ka'aihue, L., 2001. Potential for photoenhanced toxicity of spilled oil in Prince William Sound and Gulf of Alaska waters. Mar. Pollut. Bull. 43 (1–6), 86–92.

Bekins, B.A., Brennan, J.C., Tillitt, D.E., Cozzarelli, I.M., Illig, J.M., Martinović-Weigelt, D., 2020. Biological effects of hydrocarbon degradation intermediates: is the total petroleum hydrocarbon analytical method adequate for risk assessment? Environ. Sci. Technol. 54 (18), 11396–11404.

Bianchi, T.S., Osburn, C., Shields, M.R., Yvon-Lewis, S., Young, J., Guo, L., Zhou, Z., 2014. Deepwater Horizon oil in Gulf of Mexico waters after 2 years: transformation into the dissolved organic matter pool. Environ. Sci. Technol. 48 (16), 9288–9297.

BOEM, 2016. Alaska Outer Continental Shelf Cook Inlet Planning Area Oil and Gas Lease Sale 244: Final Environmental Impact Statement.

Brennan, J.C., Tillit, D.E., 2018. Development of a dual luciferase activity and fluorescamine protein assay adapted to a 384 micro-well plate format: reducing variability in human luciferase transactivation cell lines aimed at endocrine active substances. Toxicol. Vitro 47, 18–25.

Brennan, J.C., He, G., Tsutsumi, T., Zhao, J., Wirth, E., Fulton, M.H., Denison, M.S., 2015. Development of species-specific Ah receptor-responsive third generation CALUX cell lines with enhanced responsiveness and improved detection limits. Environ. Sci. Technol. 49 (19), 11903–11912.

Coelho, N.R., Pimpão, A.B., Correia, M.J., et al., 2022. Pharmacological blockage of the AHR-CYP1A1 axis: a call for in vivo evidence. J. Mol. Med. 100, 215–243.

da Silva, M.R.F., Souza, K.S., de Assis, C.R.D., Santos, M.D.V., de Oliveira, M.B.M., 2020. Biomarkers as a tool to monitor environmental impact on aquatic ecosystems. Br. J. Dev. 6 (10), 75702–75720.

D'Auria, M., Racioppi, R., Velluzzi, V., 2008. Photodegradation of crude oil: liquid injection and headspace solid-phase microextraction for crude oil analysis by gas chromatography with mass spectrometer detector. J. Chromatogr. Sci. 46 (4), 339–344.

Dawson, J., Pizzolato, L., Howell, S.E., Copland, L., Johnston, M.E., 2015. Temporal and spatial patterns of ship traffic in the Canadian Arctic from 1990 to 2015. Arctic 71 (1), 15–26.

Dissing, D., Wendler, G., 1998. Solar radiation climatology of Alaska. Theor. Appl. Climatol. 61 (3), 161–175.

Dittmar, T., Koch, B., Hertkorn, N., Kattner, G., 2008. A simple and efficient method for the solid- phase extraction of dissolved organic matter (SPE-DOM) from seawater. Limnol Oceanogr. Methods 6 (6), 230–235.

Dvorski, S.E.-M., Gonsior, M., Hertkorn, N., Uhl, J., Müller, H., Griebler, C., Schmitt-Kopplin, P., 2016. Geochemistry of dissolved organic matter in a spatially highly resolved groundwater petroleum hydrocarbon plume cross-section. Environ. Sci. Technol. 50 (11), 5536–5546.

Essaid, H.I., Bekins, B.A., Herkelrath, W.N., Delin, G.N., 2011. Crude oil at the Bemidji site: 25 years of monitoring, modeling, and understanding. Ground Water 49 (5), 706–726.

Fan, J., Sun, X., Liu, Y., Zhao, D., Hao, X., Liu, W., Cai, Z., 2022. New insight into environmental photochemistry of PAHs induced by dissolved organic matters: a model of naphthalene in seawater. Process Saf. Environ. Protect. 161, 325–333.

Fedi, L., Faury, O., Etienne, L., 2020. Mapping and analysis of maritime accidents in the Russian Arctic through the lens of the Polar Code and POLARIS system. Mar. Pol. 118, 103984.

Freeman, D.H., Niles, S.F., Rodgers, R.P., French-McCay, D.P., Longnecker, K., Reddy, C. M., Ward, C.P., 2023. Hot and cold: photochemical weathering mediates oil properties and fate differently depending on seawater temperature. Environ. Sci. Technol. 57 (32), 11988–11998.

Gaber, M., Al Sequely, A., Monem, N.A., Balbaa, M., 2021. Effect of polyaromatic hydrocarbons on cellular cytochrome P450 1A induction. Ocean and Coastal Research v69, e21026.

Garrett, R.M., Pickering, I.J., Haith, C.E., Photooxidation, R.C., 1998. Of crude oils. Prince Environmental Science & Technology 32 (23), 3719–3723.

Goetz, K.T., Montgomery, R.A., Ver Hoef, J.M., Hobbs, R.C., Johnson, D.S., 2012. Identifying essential summer habitat of the endangered beluga whale Delphinapterus leucas in Cook Inlet, Alaska. Endanger. Species Res. 16 (2), 135–147.

Grosse, S., Letzel, T., 2007. Liquid chromatography/atmospheric pressure ionization mass spectrometry with post-column liquid mixing for the efficient determination of partially oxidized polycyclic aromatic hydrocarbons. J. Chromatogr. A 1139 (1), 75–83.

Harsha, M.L., Redman, Z.C., Wesolowski, J., Podgorski, D.C., Tomco, P.L., 2023. Photochemical formation of water-soluble oxyPAHs, naphthenic acids, and other hydrocarbon oxidation products from Cook Inlet, Alaska crude oil and diesel in simulated seawater spills. Environ. Sci. J. Integr. Environ. Res.: Advances 2, 447–461.

Hazen, T.C., Prince, R.C., Mahmoudi, N., 2016. Marine Oil Biodegradation. ACS Publications.

Hood, D.W., Zimmerman, S.T., 1987. Gulf of Alaska: Physical Environment and Biological Resources. National Ocean Service, Anchorage, AK (USA). Ocean Assessments Div.

Kapsar, K., Gunn, G., Brigham, L., et al., 2023. Mapping vessel traffic patterns in the ice-covered waters of the Pacific Arctic. Climatic Change 176. https://doi.org/10.1007/s10584-023-03568-3.

Knecht, A.L., Goodale, B.C., Truong, L., Simonich, M.T., Swanson, A.J., Matzke, M.M., Anderson, K.A., Waters, K.M., Tanguay, R.L., 2013. Comparative developmental toxicity of environmentally relevant oxygenated PAHs. Toxicol. Appl. Pharmacol. 271 (2), 266–275.

Koch, B.P., Dittmar, T., 2006. From mass to structure: an aromaticity index for high-resolution mass data of natural organic matter. Rapid Commun. Mass Spectrom. 20 (5), 926–932.

Krüger, O., Kalbe, U., Meißner, K., Sobottka, S., 2014. Sorption effects interfering with the analysis of polycyclic aromatic hydrocarbons (PAH) in aqueous samples. Talanta 122, 151–156.

Lampi, M.A., Gurska, J., McDonald, K.I., Xie, F., Huang, X.D., Dixon, D.G., Greenberg, B. M., 2006. Photoinduced toxicity of polycyclic aromatic hydrocarbons to Daphnia magna: ultraviolet- mediated effects and the toxicity of polycyclic aromatic hydrocarbon photoproducts. Environ. Toxicol. Chem. 25 (4), 1079–1087.

Lee, R., 2003. Photo-oxidation and photo-toxicity of crude and refined oils. Spill Sci. Technol. Bull. 8 (2), 157–162.

Lunel, T., 1998. Sea Empress spill: dispersant operations, effectiveness and effectiveness monitoring. Proceedings of the Dispersant Use in Alaska: A Technical Update, pp. 59–78.

Luo, H., Chen, J., Li, G., An, T., 2021. Formation kinetics and mechanisms of ozone and secondary organic aerosols from photochemical oxidation of different aromatic hydrocarbons: dependence on NO_x and organic substituents. Atmos. Chem. Phys. 21 (10), 7567–7578.

McDonnell, A.M., Dang, C.H., 2013. Basic review of the cytochrome p450 system. J Adv Pract Oncol 4 (4), 263–268.

McFarlin, K.M., Prince, R.C., Perkins, R., Leigh, M.B., 2014. Biodegradation of dispersed oil in arctic seawater at-1 C. PLoS One 9 (1), E84297.

Mennillo, E., Adeogun, A.O., Arukwe, A., 2020. Quality screening of the Lagos lagoon sediment by assessing the cytotoxicity and toxicological responses of rat hepatoma H4IIE and fish PLHC-1 cell-lines using different extraction approaches. Environ. Res. 182, 108986.

Mirnaghi, F.S., Pinchin, N.P., Yang, Z., Hollebone, B.P., Lambert, P., Brown, C.E., 2019. Monitoring of polycyclic aromatic hydrocarbon contamination at four oil spill sites using fluorescence spectroscopy coupled with parallel factor-principal component analysis. Environ. Sci. J. Integr. Environ. Res.: Process. Impacts 21 (3), 413–426.

Mohler, R.E., Ahn, S., O'Reilly, K., Zemo, D.A., Devine, C.E., Magaw, R., Sihota, N., 2020. Towards comprehensive analysis of oxygen containing organic compounds in groundwater at a crude oil spill site using GC× GC-TOFMS and Orbitrap ESI-MS. Chemosphere 244, 125504.

Nakano, N., Sakata, N., Katsu, Y., Nochise, D., Sato, E., Takahashi, Y., Yamaguchi, S., Haga, Y., Ikeno, S., 2020. Composition and fate of petroleum and spill-treating agents in the marine environment.

Neff, J.M., 1988. Composition and fate of petroleum and spill-treating agents in the marine environment. In: Geraci, J.R., Aubin, D.J. St (Eds.), Sea Mammals and Oil: Confronting the Risks. Academic, San Diego, USA, pp. 1–34.

Nguyen, V.H., Thi, L.A.P., Van Le, Q., Singh, P., Raizada, P., Kajitvichyanukul, P., 2020. Tailored photocatalysts and revealed reaction pathways for photodegradation of polycyclic aromatic hydrocarbons (PAHs) in water, soil and other sources. Chemosphere 260, 127529.

Pizzolato, L., Howell, S.E., Derksen, C., Dawson, J., Copland, L., 2014. Changing sea ice conditions and marine transportation activity in Canadian Arctic waters between 1990 and 2012. Climatic Change 2014 (123), 161–173.

Redman, Z.C., Wesolowski, J., Tomco, P.L., 2021. Photochemical pathways of rotenone and deguelin degradation: implications for rotenoid attenuation and persistence in high-latitude lakes. Environ. Sci. Technol. 55 (8), 4974–4983.
Royer, T.C., Grosch, C.E., 2006. Ocean warming and freshening in the northern Gulf of Alaska. Geophys. Res. Lett. 33 (16).
Spies, R.B., 2006. Long-term Ecological Change in the Northern Gulf of Alaska. Elsevier.
Townsend, G.T., Prince, R.C., Suflita, J.M., 2003. Anaerobic oxidation of crude oil hydrocarbons by the resident microorganisms of a contaminated anoxic aquifer. Environ. Sci. Technol. 37 (22), 5213–5218.
USEPA, 1996a. *Method 8015B: Nonhalogenated Organics Using GC-FID.* SW-846 Revision, p. 2.
USEPA, 1996b. Separatory Funnel Liquid-Liquid Extraction.
USEPA, 2000. METHOD 8015C NONHALOGENATED ORGANICS USING GC/FID.
Ward, C.P., Sharpless, C.M., Valentine, D.L., French-McCay, D.P., Aeppli, C., White, H.K., Rodgers, R.P., Gosselin, K.M., Nelson, R.K., Reddy, C.M., 2018. Partial photochemical oxidation was a dominant fate of Deepwater Horizon surface oil. Environ. Sci. Technol. 52 (4), 1797–1805.
Weingartner, T.J., Coyle, K., Finney, B., Hopcroft, R., Whitledge, T., Brodeur, R., Dagg, M., Farley, E., Haidvogel, D., Royer, T., 2002. The northeast Pacific GLOBEC program: coastal Gulf of Alaska. Oceanography 15 (2).
Whisenhant, E.A., Zito, P., Podgorski, D.C., McKenna, A.M., Redman, Z.C., Tomco, P.L., 2022. Unique molecular features of water-soluble photo-oxidation products among refined fuels, crude oil, and herded burnt residue under high latitude conditions. ACS ES&T water. Whitney, J., Cook Inlet, Alaska: oceanographic and ice conditions and NOAA's 18-year oil spill response history 1984-2001 2 (6), 994–1002, 2002.
Wölz, J., Brack, W., Moehlenkamp, C., Claus, E., Braunbeck, Th, Hollert, H., 2010. Effect-directed analysis of Ah receptor-mediated activities caused by PAHs in suspended particulate matter sampled in flood events. Sci. Total Environ. 408 (16), 3327–3333.
Yang, X., Cai, H., Bao, M., Yu, J., Lu, J., Li, Y., 2018. Insight into the highly efficient degradation of PAHs in water over graphene oxide/Ag3PO4 composites under visible light irradiation. Chem. Eng. J. 334, 355–376.
Zemo, D.A., O'Reilly, K.T., Mohler, R.E., Tiwary, A.K., Magaw, R.I., Synowiec, K.A., 2013. Nature and estimated human toxicity of polar metabolite mixtures in groundwater quantified as TPHd/DRO at biodegrading fuel release sites. Groundwater Monitoring & Remediation 33 (4), 44–56.
Zhang, Z., Huisingh, D., Song, M., 2019. Exploitation of trans-Arctic maritime transportation. J. Clean. Prod. 212, 960–973.
Zhou, Z., Guo, L., Shiller, A.M., Lohrenz, S.E., Asper, V.L., Osburn, C.L., 2013. Characterization of oil components from the Deepwater Horizon oil spill in the Gulf of Mexico using fluorescence EEM and PARAFAC techniques. Mar. Chem. 148, 10–21.
Zito, P., Ghannam, R., Bekins, B.A., Podgorski, D.C., 2019a. Examining the extraction efficiency of petroleum-derived dissolved organic matter in contaminated groundwater plumes. Groundwater Monitoring & Remediation 39 (4), 25–31.
Zito, P., Podgorski, D.C., Johnson, J., Chen, H., Rodgers, R.P., Guillemette, F., Kellerman, A.M., Spencer, R.G., Tarr, M.A., 2019b. Molecular-level composition and acute toxicity of photosolubilized petrogenic carbon. Environ. Sci. Technol. 53 (14), 8235–8243.
Zito, P., Podgorski, D.C., Bartges, T., Guillemette, F., Roebuck Jr., J.A., Spencer, R.G., Rodgers, R.P., Tarr, M.A., 2020. Sunlight-induced molecular progression of oil into oxidized oil soluble species, interfacial material, and dissolved organic matter. Energy Fuels 34 (4), 4721–4726.